

The Effect of Automatic Gain Control on Serial, Matched-Filter Acquisition in Direct-Sequence Packet Radio Communications

Daniel L. Noneaker, *Member, IEEE*, Arvind R. Raghavan, and Carl W. Baum, *Member, IEEE*

Abstract—The performance of a noncoherent serial acquisition technique is evaluated for direct-sequence spread-spectrum packet communications. The acquisition technique that is considered uses threshold crossing of a matched-filter output to detect a fixed-length preamble at the start of each packet. The analysis accounts for frequency mismatch between the transmitter and the receiver due to oscillator inaccuracies and mobility-induced Doppler shifts. It also accounts for the effects of automatic gain control (AGC) in the receiver. The role of the AGC system in determining the acquisition performance is examined. In addition, selection of the optimal acquisition threshold is considered, and a simple method for selection of a good suboptimal threshold is presented. It is shown that use of this threshold results in performance close to that obtained with the optimal threshold over a wide range of channels.

Index Terms—Packet radio, pseudonoise coded communication, radio receivers, synchronization.

I. INTRODUCTION

DIRECT-sequence (DS) spread-spectrum modulation has found widespread application in both commercial and military communications because of the unique combination of multiple-access capability, multipath-discrimination capability, and anti-jam capability that it provides. It is employed currently in cellular code-division multiple-access (CDMA) networks [1] and personal-communication networks, and it has been proposed for use in tactical radio networks for the military [2]. The increase in data traffic in cellular networks motivates the use of random-access packet data communications on the reverse link of a CDMA network, and packet radio communications is necessary to achieve robustness in a DS distributed, tactical military network.

Successful reception of a DS packet transmission requires that the receiver synchronize the spreading sequence [3] of the arriving packet with a locally generated copy of the same sequence. The process of synchronization is usually performed in

two stages: acquisition and tracking [4]. The *a priori* timing uncertainty of the arriving signal may be very large, and the acquisition stage is intended to obtain coarse alignment between the local sequence and the sequence of the arriving signal [5]. Acquisition can be the limiting factor in the performance of a DS spread-spectrum multiple-access communications system [6], and the choice of acquisition technique is critical to achieving acceptable performance in a DS system employing random-access packet radio communications. It is the design and performance of the acquisition stage for DS packet radio communications that we consider in this paper.

A number of techniques have been proposed for serial acquisition of a DS signal. (See [4] for an overview.) Some techniques employ an active, programmable correlator that is used to test sequentially for possible signal delays [5]. Active-correlation techniques are attractive because of their simple implementation, but they often require observation of the signal for a relatively long period of time in order to acquire the signal. Thus, they are well suited for use in a connection-oriented system in which the data signal or a pilot signal is present continuously over an extended period of time. But they are ill suited for use with DS packet radio communications in which each packet must be acquired only from observation of a short acquisition preamble. Instead, acquisition techniques that employ a passive filter that is matched to the sequence in the acquisition preamble [7], [8] are better suited to DS packet radio communications. It is the latter technique that is considered here.

In this paper, we analyze the performance of a noncoherent serial acquisition technique for use in DS packet radio communications. Passive in-phase and quadrature filters are matched to the spreading sequence used in the acquisition preamble of the transmitted packet. Each square-law output of the noncoherent detector is compared to a threshold to detect synchronization with the received signal. In a mobile environment, the power in the signal can vary over a large range at the receiver, and the receiver must employ gain control to ensure acceptable performance of its subsystems. The analysis presented here accounts for the effects of an automatic gain control (AGC) system, and the AGC system together with its preceding bandpass filter is shown to play an important role in acquisition performance. In addition, mobility-induced Doppler shifts and oscillator inaccuracies typically result in differences between the carrier frequency of the received transmission and the reference frequency employed by the receiver during the acquisition stage. The analysis accounts for the effects of this frequency mismatch as well. Previous papers [9], [10] have addressed the effect of Doppler

Manuscript received April 2, 1999; revised November 29, 2000. This work was supported by the Office of Naval Research under Grants N00014-96-1-0896 and N00014-00-1-0565 and by the Army Research Office under Grants DAAH04-95-1-0247 and DAAD19-00-1-0156. It was presented in part at the 1998 IEEE International Conference on Communications, Atlanta, GA, June 1998.

D. L. Noneaker and C. W. Baum are with the Department of Electrical and Computer Engineering, Clemson University, Clemson, SC 29634-0915 USA (e-mail: dann0@ces.clemson.edu; baum@ces.clemson.edu).

A. R. Raghavan is with OPNET Technologies, Inc., Washington, DC 20008 USA (e-mail: araghavan@opnet.com).

Publisher Item Identifier S 0018-9545(01)04886-1.

shift on the performance of DS acquisition. But they do not consider matched-filter acquisition, and they do not account for the effects of gain control in the receiver.

This paper is organized as follows. In Section II, the transmitted signal, the channel, the AGC system, and the acquisition stage are described. The relationship among the spectrum of the DS signal, the transfer function of the bandpass filter, and the response of the AGC system is considered in Section III. An analysis of the performance of the serial, matched-filter acquisition technique is presented in Section IV. The effect of the bandpass filter and AGC system on acquisition performance is examined in Section V, and some surprising behavior is revealed. In Section VI, selection of the optimal acquisition threshold is addressed, and a simple method for finding a good suboptimal threshold is developed. The performance resulting from the use of this threshold is compared with the performance resulting from the use of the optimal threshold.

II. SYSTEM DESCRIPTION

A. Transmitted Signal and Received Signal

The packet transmission employs DS spread-spectrum modulation and consists of an acquisition preamble of length M chips followed by the packet's data content. The preamble is transmitted during the time interval $[0, MT_c]$, and the data content is transmitted during the time interval $[MT_c, (M+L)T_c]$, where T_c is the duration of a chip in the DS spread-spectrum waveform. The transmission voltage into a nominal $1\text{-}\Omega$ load is given by

$$s(t) = \sqrt{2} \mathcal{R}e \left\{ \tilde{s}(t) e^{j(2\pi f_c t)} \right\}$$

where

$$\tilde{s}(t) = \sqrt{P} c(t) [p_{MT_c}(t) + d(t)p_{LTC}(t - MT_c)] \quad (1)$$

f_c is the carrier frequency at the transmitter, P is the power in the transmitted signal during the preamble, $p_T(t)$ is the unit-height rectangular pulse over $[0, T)$, and $d(t)$ is the signal representing the data content of the packet. The specific format of $d(t)$ is not relevant to the development in this paper.

The quaternary phase-shift-keyed (QPSK) spreading waveform [3] is given by

$$c(t) = \sum_{i=0}^{M+L-1} a_i \psi(t - iT_c)$$

where $\{a_i\}$ represents a complex-valued spreading sequence [3], which takes on values in $\{e^{j(\pi/4)}, e^{j(3\pi/4)}, e^{j(5\pi/4)}, e^{j(7\pi/4)}\}$. The spreading sequence is modeled as a sequence of independent, identically distributed, complex-valued random variables that are uniformly distributed over the four values. This *random-sequence* model [11] provides a good approximation to the use of distinct binary-valued long-period pseudonoise sequences for generation of the real and imaginary parts of the complex-valued spreading sequence. The chip

waveform $\psi(t)$ is time limited to $[0, T_c)$. From the definition of $s(t)$ and $c(t)$, it follows that

$$\frac{1}{T_c} \int_{t=0}^{T_c} |\psi(t)|^2 dt = 1. \quad (2)$$

Without loss of generality, the transmitted signal is assumed to arrive unattenuated and undelayed at the receiver over an additive white Gaussian noise channel. As a result of oscillator inaccuracies and the mobility of the transmitter and the receiver, the receiver-generated reference frequency f_r can differ from the carrier frequency of the received signal. The difference, denoted f_d , is assumed to be constant over the duration of the preamble. Thus the received signal voltage into a nominal $1\text{-}\Omega$ load is given by

$$r(t) = \sqrt{2} \mathcal{R}e \left\{ \tilde{r}(t) e^{j(2\pi f_r t)} \right\} \quad (3)$$

where

$$\tilde{r}(t) = \tilde{s}(t) e^{j2\pi f_d t + \theta_0} + \tilde{n}(t) \quad (4)$$

and θ_0 is a constant. The complex-valued, baseband-equivalent white-Gaussian-noise voltage process $\tilde{n}(t)$ has two-sided power spectral density N_0 , so that the power spectral density is $N_0/2$ in each of its real and imaginary parts. The dimensionless (normalized) *Doppler shift* of the received signal is defined as

$$D_{T_c} = f_d T_c.$$

B. Receiver Architecture

A typical heterodyne receiver consists of a radio-frequency (RF) stage that first amplifies and then converts the received signal to an intermediate frequency (IF), an IF bandpass filter, an AGC system, an analog-to-digital (A/D) converter, demodulation to baseband, and subsequent digital signal processing [12]. In some heterodyne receivers, the order of the A/D conversion and the mixing to baseband are reversed. In either case, the AGC system serves to maintain the proper voltage range at the input to the A/D converter, and it may also be used with a feedback loop to ensure that the RF-stage amplifier does not drive the RF mixer into compression. The IF filter rejects out-of-band noise power before the AGC system and can serve as an anti-aliasing filter for the A/D conversion.

The thermal noise introduced in the RF-stage amplifier, the transfer function of the IF filter, and the action of the AGC system can have a significant effect on the performance of the acquisition algorithm that is implemented in the signal processing. This effect is the focus of this paper. Thus neither the demodulation from RF to IF in the receiver nor the A/D conversion are modeled explicitly. Instead, the signal given in (3) is taken as the received signal after demodulation to IF so that f_r is the local-reference intermediate frequency. The receiver is modeled as an AWGN source, a bandpass IF filter, and an AGC system followed by an acquisition stage based on processing of the unquantized continuous-time signal.

The impulse response of the IF filter is given by

$$h(t) = 2 \mathcal{R}e \left\{ \tilde{h}(t) e^{j(2\pi f_r t)} \right\}$$

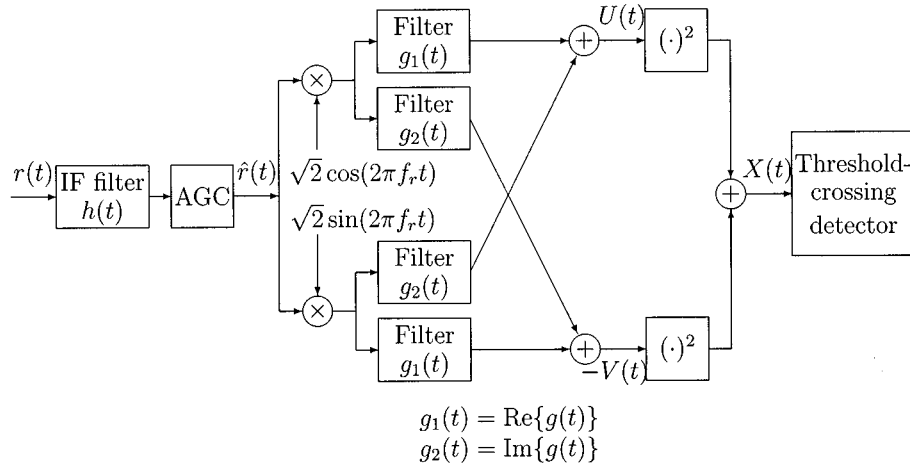


Fig. 1. Block diagram of the acquisition stage.

where $\tilde{h}(t)$ is the baseband-equivalent impulse response of the filter. Without loss of generality, we assume that

$$\max_f |\tilde{H}(f)| = |H(f)| = 1$$

where $H(f)$ is the frequency response of the IF filter and $\tilde{H}(f)$ is the baseband-equivalent frequency response. Filters with integrable power-transfer functions are considered, so that

$$\int_{-\infty}^{+\infty} |\tilde{H}(f)|^2 df = \int_{-\infty}^{+\infty} |\tilde{h}(t)|^2 dt < \infty.$$

A properly designed AGC system responds to step changes in the average input power within a fraction of the duration of the acquisition preamble and achieves minimal variation in its average output power over a wide dynamic range for the input power. In this paper, we approximate such a design by considering an AGC system that responds instantly to a step change in the average steady-state input power and maintains a constant average steady-state output power. Thus the signal at the output of the AGC system $\hat{r}(t)$ is given by

$$\hat{r}(t) = \sqrt{\alpha(t)} (r * h)(t) \quad (5)$$

where $1/\alpha(t)$ is the average steady-state power at the input of the AGC system at time t and “*” denotes convolution.

C. Acquisition Algorithm

The acquisition stage employs noncoherent square-law combining of filter outputs to form the test statistics. A block diagram of the system for acquisition is shown in Fig. 1. The in-phase and quadrature branches of the receiver each contain two filters, denoted $g_1(t)$ and $g_2(t)$. The outputs in each branch at time t are summed to form

$$U(t) = \text{Re}\{(y * g)(t)\} \quad (6)$$

$$V(t) = \text{Im}\{(y * g)(t)\} \quad (7)$$

where $y(t) = \sqrt{\alpha(t)} (\tilde{r} * \tilde{h})(t)$ and $g(t) = g_1(t) + jg_2(t)$.

The test statistics $X(t) = U^2(t) + V^2(t)$ are derived from the outputs of the filters. If $X(t)$ exceeds a threshold at time t_0 , a hit is declared, and the receiver determines the time t_1 , $t_0 \leq t_1 \leq$

$t_0 + T_c$, for which $X(t)$ is largest. A locally generated copy of the spreading waveform is then synchronized to the delay $t_1 - MT_c$, and the waveform is used in a correlator to demodulate the data symbols.

In a digital implementation of the receiver, $X(t)$ is sampled at an integer multiple of the chip rate, yielding multiple samples per chip interval. If a hit is declared, subsequent samples occurring within T_c of the sample resulting in the hit are examined to determine synchronization of the correlator. The resulting timing uncertainty at the receiver is small, provided there are a sufficient number of samples per chip. The performance of this technique can be approximated by considering a model in which the detector output is sampled only once per chip interval to produce a single test statistic for the chip interval and in which the received signal is chip synchronous with the sampling times. The latter model is used in the analysis.

If the detector fails to declare a hit until after the end of a packet's acquisition preamble, a *miss* occurs and the packet is not acquired. Conversely, if the detector declares a hit at least one chip interval before the end of the preamble, a *false alarm* occurs. A finite amount of time is required for the receiver to detect the occurrence of a false alarm so that the receiver can return to the acquisition mode. If the end of the preamble arrives during this *false-alarm processing interval*, the packet is not acquired.

The duration of the false-alarm processing interval depends on the design of the system. There are numerous techniques for the verification of DS signal acquisition [4], though many of them are not suitable for use with a packet transmission containing a fixed-length acquisition preamble. In the simplest implementation, the receiver must demodulate and decode for the duration of an entire packet and determine that cyclic-redundancy-check decoder failure has occurred in order to detect that a false alarm has occurred. In this case, the false-alarm processing interval is equal to the duration of the data portion of a packet. In other implementations, the receiver may employ information from a data-directed tracking loop [4] in order to determine that a false alarm has occurred. In this case, the false-alarm processing interval may be variable. In yet other implementations, the preamble of each packet is followed by

a start-of-frame delimiter, and the duration of the false-alarm processing interval can be as short as the time required to demodulate and detect an invalid delimiter. Thus depending on the system's design, the false-alarm processing interval can have either constant or random duration, and it can be much shorter or much longer than the duration of the preamble. The focus of this paper is not on the verification technique, and we limit our attention to systems with a constant false-alarm processing interval for convenience. A false-alarm processing interval of arbitrary constant duration is considered in the analysis.

The filters for the acquisition stage that are considered in the analysis are those having the form

$$g(t) = \sum_{i=0}^{M-1} a_{M-1-i}^* \varphi(t - iT_c).$$

(Recall that $\{a_0, \dots, a_{M-1}\}$ is the spreading sequence for the acquisition preamble.) Furthermore, the impulse response of the baseband-equivalent IF filter $\tilde{h}(t)$ and the function $\varphi(t)$ that are considered satisfy the joint constraint

$$\left(\tilde{h} * \varphi\right)(t) = \psi^*(T_c - t), \quad \text{for all } t. \quad (8)$$

Under this constraint, the convolution of the IF filter's baseband-equivalent impulse response with the complex-valued filter in the acquisition stage is matched to the acquisition preamble in the DS signal. Two special cases of this receiver are considered. In one case, the IF filter introduces no distortion of the DS signal and $\varphi(t) = \psi^*(T_c - t)$. Thus

$$g(t) = c^*(MT_c - t), \quad 0 \leq t \leq MT_c$$

which is the standard realization of a filter matched to the preamble. In the second case, the baseband-equivalent IF filter $\tilde{h}(t)$ is matched to the chip waveform, so that

$$g(t) = \sum_{i=0}^{M-1} a_{M-1-i}^* \delta(t - iT_c). \quad (9)$$

The differing performance for the two matched-filter implementations is due solely to the difference in the AGC amplification that results with the two implementations. Constraints on the cost and complexity of the IF filter may preclude matching it to the chip waveform as in the latter implementation, but nonetheless, it is instructive to consider the performance that results.

III. THE EFFECT OF THE IF FILTER RESPONSE ON THE AGC AMPLIFICATION

For a given input signal power and thermal noise power density, the transfer function of the IF filter determines the power at the input to the AGC system. In most land-mobile communications and for reasonable oscillator tolerances, the largest possible value of f_d in (4) is a small fraction of the signal bandwidth. (That is, $D_{T_c} \ll 1$.) Thus, the Doppler shift has negligible effect on the power at the output of the IF filter, and its effect is ignored in the development in this section. We consider IF filters that are causal.

Consider the time interval $[kT_c, (k+1)T_c]$, $0 \leq k < M$, corresponding to the k th chip in the preamble of the DS signal.

The average power at the input to the AGC system (i.e., at the output of the IF filter) over the interval is given by

$$\begin{aligned} & E \left[\frac{1}{T_c} \int_{t=kT_c}^{(k+1)T_c} [(r * h)(t)]^2 dt \right] \\ &= E \left[\frac{1}{T_c} \int_{t=kT_c}^{(k+1)T_c} |(\tilde{r} * \tilde{h})(t)|^2 dt \right] \\ &= \frac{P}{T_c} \int_{t=kT_c}^{(k+1)T_c} E \left[\left| \sum_{i=0}^k a_i (\psi * \tilde{h})(t - iT_c) \right|^2 \right] dt \\ &\quad + \frac{1}{T_c} \int_{t=kT_c}^{(k+1)T_c} E \left[|(\tilde{n} * \tilde{h})(t)|^2 \right] dt \end{aligned} \quad (10)$$

$$\begin{aligned} &= \frac{P}{T_c} \sum_{i=0}^k \int_{t=kT_c}^{(k+1)T_c} |(\psi * \tilde{h})(t - iT_c)|^2 dt \\ &\quad + \frac{1}{T_c} \int_{t=kT_c}^{(k+1)T_c} E \left[|(\tilde{n} * \tilde{h})(t)|^2 \right] dt \end{aligned} \quad (11)$$

$$= \frac{P}{T_c} \int_0^{(k+1)T_c} |(\psi * \tilde{h})(t)|^2 dt + \int_{-\infty}^{+\infty} N_0 |\tilde{h}(\tau)|^2 d\tau. \quad (12)$$

The baseband-equivalent IF filters of interest have rise times no more than one or two times the chip duration, so that within a few chips of the start of the preamble, the average power at the output of the IF filter approaches a steady-state value expressed by

$$\begin{aligned} & E \left[\frac{1}{T_c} \int_{t=kT_c}^{(k+1)T_c} [(r * h)(t)]^2 dt \right] \\ &\approx \frac{P}{T_c} \int_0^{+\infty} |(\psi * \tilde{h})(t)|^2 dt + \int_{-\infty}^{+\infty} N_0 |\tilde{h}(\tau)|^2 d\tau \\ &= \frac{P}{T_c} \int_{-\infty}^{+\infty} |\Psi(f)|^2 |\tilde{H}(f)|^2 df + N_0 \int_{-\infty}^{+\infty} |\tilde{H}(f)|^2 df \end{aligned} \quad (13)$$

where $\Psi(f)$ is the Fourier transform of $\psi(t)$. The first term in (13) corresponds to the average signal power at the output of the IF filter and the second term corresponds to the noise power at the output of the IF filter. The step from (10) to (11) follows from the fact that $E[a_i a_j^*] = 0$, for $i \neq j$, and that $E[|a_i^*|^2] = 1$, for all i .

The fraction of the signal power that is passed through the IF filter is given by the unitless parameter

$$\begin{aligned} \gamma_s &= \frac{\frac{P}{T_c} \int_{-\infty}^{+\infty} |\Psi(f)|^2 |\tilde{H}(f)|^2 df}{P} \\ &= \int_{-\infty}^{+\infty} \frac{|\Psi(f)|^2}{T_c} |\tilde{H}(f)|^2 df. \end{aligned} \quad (14)$$

Let the unitless parameter γ_n represent the ratio of the noise power passed through the IF filter to the noise power that would pass through an ideal unity-gain bandpass filter with single-sided baseband-equivalent bandwidth $1/2T_c$. Then

$$\gamma_n = \frac{N_0 \int_{-\infty}^{+\infty} |\tilde{H}(f)|^2 df}{N_0 \left(\frac{1}{T_c}\right)} = T_c \int_{-\infty}^{+\infty} |\tilde{H}(f)|^2 df. \quad (15)$$

Thus, from (13)–(15), the steady-state average power at the input to the AGC system during the reception of the preamble can be expressed as

$$E \left[\frac{1}{T_c} \int_{t=kT_c}^{(k+1)T_c} [(r * h)(t)]^2 dt \right] = \gamma_s \left(P + \beta \frac{N_0}{T_c} \right) \quad (16)$$

where

$$\beta = \gamma_n / \gamma_s$$

is also a unitless parameter. Note that γ_s , γ_n , and β depend only on the chip waveform and the transfer function of the IF filter and that they do not depend on the signal power or the noise power spectral density.

Similarly, the average power at the input to the AGC system before the arrival of the DS signal is given by

$$E \left[\frac{1}{T_c} \int_{t=kT_c}^{(k+1)T_c} [(\tilde{n} * \tilde{h})(t)]^2 dt \right] = \gamma_n \frac{N_0}{T_c} = \gamma_s \beta \frac{N_0}{T_c} \quad (17)$$

for $k < 0$.

We make the approximation that the output of the AGC system settles to its new steady-state power instantly upon arrival of the DS signal. Thus the amplification resulting from the AGC system is determined by (5) with

$$\alpha(t) = \begin{cases} \alpha_0 = \left(\gamma_s \beta \frac{N_0}{T_c} \right)^{-1}, & t < 0 \\ \alpha_1 = \gamma_s^{-1} \left(P + \beta \frac{N_0}{T_c} \right)^{-1}, & 0 \leq t \leq MT_c. \end{cases} \quad (18)$$

By Parseval's theorem, it follows from (2) that

$$\int_{-\infty}^{+\infty} |\Psi(f)|^2 df = \int_0^{T_c} |\psi(t)|^2 dt = T_c. \quad (19)$$

Since $|\tilde{H}(f)| \leq 1$ for all f , it thus follows from (14) and (19) that the value of γ_s can be no greater than one, and $\gamma_s = 1$ if and only if $|\tilde{H}(f)| = 1$ for all f such that $\Psi(f) \neq 0$. But the latter condition is impossible if the chip waveform is time limited and the filter has an integrable power-transfer function. Thus $\gamma_s < 1$. A further constraint is obtained by noting that

$$\int_{t=0}^{T_c} (|\psi(t)| - 1)^2 dt \geq 0 \quad (20)$$

with equality if and only if $|\psi(t)|$ is identically equal to one on $[0, T_c)$. From (2) and (20), it follows that

$$\int_{-\infty}^{+\infty} |\psi(t)| dt = \int_{t=0}^{T_c} |\psi(t)| dt \leq T_c$$

with equality if and only if $|\psi(t)|$ is identically equal to one on $[0, T_c)$. Thus

$$\begin{aligned} \max_f |\Psi(f)| &= \max_f \left| \int_{-\infty}^{+\infty} \psi(t) e^{-j2\pi ft} dt \right| \\ &\leq \int_{-\infty}^{+\infty} |\psi(t)| dt \leq T_c. \end{aligned}$$

So

$$\begin{aligned} \gamma_s &= \frac{1}{T_c} \int_{-\infty}^{+\infty} |\Psi(f)|^2 |\tilde{H}(f)|^2 df \\ &\leq \frac{1}{T_c} \int_{-\infty}^{+\infty} T_c^2 |\tilde{H}(f)|^2 df \\ &= T_c \int_{-\infty}^{+\infty} |\tilde{H}(f)|^2 df = \gamma_n \end{aligned}$$

with equality if and only if $|\Psi(f)| = T_c$ for all f such that $\tilde{H}(f) \neq 0$. Thus $\beta \geq 1$, with the same condition for equality. In fact, since $c(t)$ is time limited, it can be shown that the equality condition is never met and thus $\beta > 1$.

One implementation of the receiver in Fig. 1 that is of interest employs an IF filter that introduces minimal distortion in the received signal and a filter $g(t)$ in the acquisition stage that is matched to the DS signal in the preamble. A necessary condition for the IF filter to be essentially nondistorting is that $|\tilde{H}(f)| \approx 1$ over a range of frequencies containing most of the energy in $\Psi(f)$. From (14), it follows that $\gamma_s \approx 1$ under that condition and thus $\beta \approx \gamma_n$ and $\gamma_n > 1$. To illustrate this, consider the chip waveform given by the time-limited raised-cosine pulse

$$\psi(t) = \sqrt{\frac{2}{3}} \left[1 - \cos \left(\frac{2\pi t}{T_c} \right) \right], \quad 0 \leq t < T_c \quad (21)$$

which has a single-sided 95%-power bandwidth of $1.115/T_c$. Suppose that the IF filter is a Butterworth filter of order N with a single-sided baseband-equivalent cutoff frequency of f_B . If $N \geq 3$, then

$$2T_c f_B < \gamma_n \leq 2.1T_c f_B.$$

For example, consider a sixth-order Butterworth IF filter with a cutoff frequency of $f_B = 1.25/T_c$. The filter's phase response exhibits a maximal deviation from linearity of less than 10° over the 95%-power spectral band of the DS signal and a maximal variation in the magnitude response over the same band that is less than 0.15 dB [13]. If instead the cutoff frequency of the filter is $f_B = 1.5/T_c$, the maximal phase deviation and magnitude variation are less than 4° and 0.02 dB, respectively, over the same band. In either case, $\gamma_s \approx 1$ and the IF filter is accurately approximated as one that does not distort the DS signal. For the narrower of the two filter bandwidths $\gamma_n \approx 2.5$, and for the wider bandwidth $\gamma_n \approx 3.0$. Thus, the corresponding values of β are also approximately 2.5 and 3.0.

The second implementation of the receiver in Fig. 1 that is of interest occurs if the IF filter is matched to the chip waveform and the filter $g(t)$ in the acquisition stage is given by (9). We consider two specific examples. In the first, the IF filter is matched to a chip waveform that is a rectangular pulse. The three parameters of interest are given by $\gamma_s = 2/3$, $\gamma_n = 1$, and $\beta = 1.5$. In the second example, the IF filter is matched to a chip waveform that is the time-limited raised-cosine pulse given by (21). For this receiver, $\gamma_s = 0.7215$, $\gamma_n = 1.5$, and $\beta = 2.08$.

In conclusion, we have shown that the effect of the IF filter's transfer function on the AGC system's amplification is determined by the values of γ_s and β through (18). The specific ex-

amples discussed above, and the corresponding values of γ_s and β , are considered again later in this paper.

IV. ANALYSIS OF ACQUISITION PERFORMANCE

In the analysis that follows, the receiver that is considered samples the outputs of the filters in Fig. 1 at times $t = iT_c$, where i is an integer, in order to form the test statistics. The duration of the false-alarm processing interval is equal to QT_c , so that successful acquisition of the signal is possible only if no false alarms occur for the Q samples immediately preceding the sample corresponding to correct synchronization with the signal. A false alarm that occurs more than Q samples prior to the correct sample does not affect the ability of the receiver to acquire the signal. The analysis applies to the receiver of Fig. 1 if the convolution of the baseband-equivalent IF filter with the filter $g(t)$ in the acquisition stage is matched to the chip waveform. A more general analysis is required if that constraint is not met, though it is a conceptually straightforward extension of the development given here.

The samples are denoted by

$$U_i \doteq U(iT_c) \quad (22)$$

$$V_i \doteq V(iT_c) \quad (23)$$

where $U(iT_c)$ and $V(iT_c)$ are given by (6) and (7) and the test statistic $X_i = U_i^2 + V_i^2$ is obtained from them in turn. If $X_i \geq \eta$ for some $i < M$, a false alarm occurs. The false alarm results in a failure to acquire the packet if $M-Q < i < M-1$. If no false alarms occur for $\{X_{(M-Q)}, \dots, X_{(M-1)}\}$ and if $X_M \geq \eta$, the packet is acquired. If $X_M < \eta$, the packet is not acquired. Since false alarms have no effect on acquisition of the signal if they occur for $i < M-Q$, we need consider only the samples $\{(U_i, V_i)\}$, $M-Q \leq i \leq M$.

As noted in the previous section, we focus on systems for which $D_{T_c} \ll 1$. Thus the Doppler shift results in a small phase rotation in the baseband-equivalent received signal over the duration of a chip interval, and the phase function is approximated accurately by a piecewise-constant function of time as

$$\begin{aligned} 2\pi f_d t + \theta_0 &= 2\pi D_{T_c} (t/T_c) + \theta_0 \\ &\approx 2\pi D_{T_c} k + \theta_0, \quad kT_c \leq t < (k+1)T_c. \end{aligned} \quad (24)$$

We employ this approximation as an equality in the development that follows.

It follows from (6)–(8) that the statistics U_i and V_i can be expressed as

$$\begin{aligned} U_i &= N_i^{(U)} + I_i^{(U)} \\ V_i &= N_i^{(V)} + I_i^{(V)} \end{aligned}$$

where $N_i^{(U)}$, $N_i^{(V)}$, $I_i^{(U)}$, and $I_i^{(V)}$ are the real-valued random variables given by

$$N_i^{(U)} + jN_i^{(V)} = \int_{iT_c - MT_c}^{iT_c} \sqrt{\alpha(t)} \tilde{n}(t) c^*(t - iT_c + MT_c) dt \quad (25)$$

$$\begin{aligned} I_i^{(U)} + jI_i^{(V)} &= \int_{iT_c - MT_c}^{iT_c} \sqrt{\alpha(t)} \tilde{s}(t) c^*(t - iT_c + MT_c) \\ &\quad \times e^{j(2\pi f_d t + \theta_0)} dt. \end{aligned} \quad (26)$$

The collection of random variables $\{I_{M-Q}^{(U)}, I_{M-Q}^{(V)}, \dots, I_M^{(U)}, I_M^{(V)}\}$ is independent of the collection of random variables $\{N_{M-Q}^{(U)}, N_{M-Q}^{(V)}, \dots, N_M^{(U)}, N_M^{(V)}\}$. It follows from (25) that

$$\{N_{M-Q}^{(U)}, N_{M-Q}^{(V)}, \dots, N_M^{(U)}, N_M^{(V)}\}$$

are independent zero-mean Gaussian random variables with

$$\begin{aligned} \text{Var}(N_i^{(U)}) &= \frac{1}{4} E \left[\left(\int_{iT_c - MT_c}^{iT_c} \sqrt{\alpha(t)} \tilde{n}(t) c^*(t - iT_c + MT_c) dt \right. \right. \\ &\quad \left. \left. + \int_{iT_c - MT_c}^{iT_c} \sqrt{\alpha(t)} \tilde{n}^*(t) c(t - iT_c + MT_c) dt \right)^2 \right] \\ &= \frac{1}{2} \int_{iT_c - MT_c}^{iT_c} \int_{iT_c - MT_c}^{iT_c} \sqrt{\alpha(t)\alpha(x)} E[\tilde{n}(t)\tilde{n}^*(x)] \\ &\quad \times E[c^*(t - iT_c + MT_c)c(x - iT_c + MT_c)] dx dt \\ &= \frac{N_0}{2} \int_{iT_c - MT_c}^{iT_c} \alpha(t) E[|c(t - iT_c + MT_c)|^2] dt \\ &= \begin{cases} \alpha_0 M N_0 T_c / 2, & i \leq 0 \\ [\alpha_0(M - i) + \alpha_1 i] N_0 T_c / 2, & 1 \leq i \leq M \end{cases} \end{aligned}$$

and $\text{Var}(N_i^{(V)}) = \text{Var}(N_i^{(U)})$.

Equation (26) can be simplified as

$$\begin{aligned} I_i^{(U)} + jI_i^{(V)} &= \sqrt{P} \int_{iT_c - MT_c}^{iT_c} \sqrt{\alpha(t)} c(t) c^*(t - iT_c + MT_c) \\ &\quad \times e^{j(2\pi f_d t + \theta_0)} dt \end{aligned} \quad (27)$$

$$\begin{aligned} &= \sqrt{P} \int_0^{\max\{0, i\}T_c} \sqrt{\alpha(t)} c(t) c^*(t - iT_c + MT_c) \\ &\quad \times e^{j(2\pi f_d t + \theta_0)} dt \end{aligned} \quad (28)$$

$$= \sqrt{\alpha_1 P} \sum_{k=0}^{\max\{0, i\}-1} a_k a_{k-i+M}^* T_c e^{j(2\pi D_{T_c} k + \theta_0)} \quad (29)$$

where the step from (27) to (28) results from the fact that $c(t) = 0$ for $t < 0$ and (29) uses the approximation in (24). Thus for $i < M$

$$E[I_i^{(U)}] = 0$$

$$\begin{aligned} \text{Var}(I_i^{(U)}) &= \alpha_1 P \sum_{k=0}^{\max\{0, i\}-1} \sum_{m=0}^{\max\{0, i\}-1} \\ &\quad \times E \left[\left(\mathcal{R}e \left\{ a_k a_{k-i+M}^* e^{j(2\pi D_{T_c} k + \theta_0)} \right\} \right) \right. \\ &\quad \left. \times \left(\mathcal{R}e \left\{ a_m a_{m-i+M}^* e^{j(2\pi D_{T_c} m + \theta_0)} \right\} \right) \right] T_c^2 \\ &= \alpha_1 P \max\{0, i\} T_c^2 / 2. \end{aligned}$$

In a similar manner, it is shown that

$$\text{Var}(I_i^{(V)}) = \text{Var}(I_i^{(U)}), \quad \text{Cov}(I_i^{(U)}, I_i^{(V)}) = 0$$

and

$$\begin{aligned} \text{Cov}(I_i^{(U)}, I_n^{(U)}) &= \text{Cov}(I_i^{(U)}, I_n^{(V)}) \\ &= \text{Cov}(I_i^{(V)}, I_n^{(V)}) = 0 \end{aligned}$$

for $i \neq n$. Note that none of the first and second moments above depends on θ_0 or D_{T_c} .

In contrast

$$\begin{aligned} E \left[I_M^{(U)} + jI_M^{(V)} \right] &= \sqrt{\alpha_1 P} T_c e^{j\theta_0} \sum_{k=0}^{M-1} e^{j2\pi D_{T_c} k} \\ &= \sqrt{\alpha_1 P} T_c e^{j[\theta_0 + \pi D_{T_c} (M-1)]} \\ &\quad \times \frac{\sin(\pi D_{T_c} M)}{\sin(\pi D_{T_c})} \end{aligned}$$

and

$$\text{Var} \left(I_M^{(U)} \right) = \text{Var} \left(I_M^{(V)} \right) = 0.$$

Thus

$$\begin{aligned} E[U_i + jV_i] &= \sqrt{\alpha_1 P} T_c e^{j[\theta_0 + \pi D_{T_c} (M-1)]} \\ &\quad \times \frac{\sin(\pi D_{T_c} M)}{\sin(\pi D_{T_c})} \delta(i - M) \end{aligned} \quad (30)$$

$$\begin{aligned} \text{Var}(U_i) &= \text{Var}(V_i) \\ &= \begin{cases} \alpha_0 M N_0 T_c / 2, & i \leq 0 \\ i \alpha_1 P T_c^2 / 2 \\ \quad + [(M - i) \alpha_0 + i \alpha_1] \\ \quad \times N_0 T_c / 2, & 1 \leq i < M \\ \alpha_1 M N_0 T_c / 2, & i = M \end{cases} \end{aligned} \quad (31)$$

and $\{U_{(M-Q)}, V_{(M-Q)}, \dots, U_M, V_M\}$ are mutually uncorrelated.

Consider any fixed-size subset of statistics $\{U(t_1), V(t_1), \dots, U(t_k), V(t_k)\}$ corresponding to fixed sampling instances $\{t_1, \dots, t_k\}$, and suppose the duration of the preamble is held constant as the chip rate of the system is increased. By straightforward application of the Cramér–Wold device and the multivariate central limit theorem [14], the fixed-sized subset converges in distribution to a collection of $2k$ jointly Gaussian random variables. On this basis, we approximate the joint distribution function of the collection of uncorrelated random variables $\{U_{(M-Q)}, V_{(M-Q)}, \dots, U_M, V_M\}$ by treating them as jointly Gaussian (and therefore independent) random variables with first and second moments given by (30) and (31). Then the test statistics (X_1, \dots, X_M) are also mutually independent. Furthermore, $X_j = U_j^2 + V_j^2$, $j = M - Q, \dots, M - 1$, are central chi-square random variables with two degrees of freedom, and $X_M = U_M^2 + V_M^2$ is a noncentral chi-square random variable with two degrees of freedom.

Acquisition occurs if and only if $X_M > \eta$ and $X_j < \eta$, $M - Q \leq j \leq M - 1$, where η is the detection threshold. The probability that a false alarm occurs during the false-alarm processing interval is given by

$$\begin{aligned} P_{\text{fa}} &= 1 - \text{P}(X_{M-1} < \eta, \dots, X_{M-Q} < \eta) \\ &= 1 - \prod_{i=M-Q}^{M-1} \left[1 - \exp\left(\frac{-\eta}{2\sigma_i^2}\right) \right] \end{aligned} \quad (32)$$

where $\sigma_i^2 = \text{Var}(U_i)$ from (31). In the subsequent sections, we refer to this more succinctly as “the probability of false alarm.”

For convenience in the subsequent exposition, a *miss* is defined as an outcome for which $X_M < \eta$, regardless of whether

or not a false alarm occurs during the false-alarm processing interval. Thus, the probability of miss is given by

$$\begin{aligned} P_{\text{miss}} &= 1 - \text{P}(X_M \geq \eta) \\ &= 1 - Q\left(\frac{\mu}{\sigma_M}, \frac{\sqrt{\eta}}{\sigma_M}\right) \end{aligned} \quad (33)$$

where $\mu = |E[U_M + jV_M]|$ from (30), $\sigma_M = \sqrt{\text{Var}(U_M)}$ from (31), and $Q(\cdot, \cdot)$ is the Marcum Q function [15].

Thus, the probability of not acquiring a packet can be expressed as

$$\begin{aligned} P_{\text{nacq}} &= 1 - \text{P}(X_M \geq \eta, X_{M-1} < \eta, \dots, X_{M-Q} < \eta) \\ &= 1 - (1 - P_{\text{miss}})(1 - P_{\text{fa}}) \\ &= P_{\text{miss}} + P_{\text{fa}} - P_{\text{miss}} P_{\text{fa}} \\ &= P_{\text{fa}} + P_{\text{miss}}(1 - P_{\text{fa}}) \\ &= P_{\text{miss}} + P_{\text{fa}}(1 - P_{\text{miss}}). \end{aligned} \quad (34)$$

V. EFFECT OF THE AGC SYSTEM ON ACQUISITION PERFORMANCE

To gain insight into the effect that the AGC system has on the performance of the acquisition algorithm, it is useful to express the parameters that determine performance explicitly in terms of the signal-to-noise ratio (SNR) of the received signal. The SNR of the acquisition preamble is defined as

$$\text{SNR} = MPT_c/N_0.$$

From (30) and (31), it follows that the parameters in (32) and (33) can be expressed as

$$\mu^2 = \left(\frac{\sin(\pi D_{T_c} M)}{\sin(\pi D_{T_c})} \right)^2 T_c^2 \frac{1}{\gamma_s \left(1 + \frac{\beta M}{\text{SNR}} \right)} \quad (35)$$

$$\begin{aligned} \sigma_M^2 &= \frac{MT_c^2}{2} \frac{\frac{M}{\text{SNR}}}{\gamma_s \left(1 + \frac{\beta M}{\text{SNR}} \right)} \\ &= \frac{MT_c^2}{2\gamma_n} \left[1 - \frac{1}{\left(1 + \frac{\beta M}{\text{SNR}} \right)} \right] \end{aligned} \quad (36)$$

and

$$\sigma_i^2 = \begin{cases} \frac{MT_c^2}{2} \frac{1}{\gamma_s \beta} = \frac{MT_c^2}{2\gamma_n}, & i \leq 0 \\ \frac{iT_c^2}{2} \frac{1 + \frac{M}{\text{SNR}}}{\gamma_s \left(1 + \frac{\beta M}{\text{SNR}} \right)} \\ \quad + \frac{(M-i)T_c^2}{2} \frac{1}{\gamma_s \beta} \\ = \frac{MT_c^2}{2\gamma_n} + \frac{iT_c^2(\beta-1)}{2\gamma_n} \\ \quad \times \left(\frac{1}{1 + \frac{\beta M}{\text{SNR}}} \right), & 1 \leq i \leq M-1. \end{cases} \quad (37)$$

Recall from Section III that $\gamma_s \leq 1$ and $\beta \geq 1$. Note also that μ^2 , σ_m^2 , and σ_u^2 depend on γ_s and β only as a result of the scaling produced by the AGC system.

The probability of false alarm is determined by the value of σ_i^2 for $i \leq M-1$. From (37), the parameter σ_i^2 does not depend on SNR for $i \leq 0$. But if $\beta > 1$, the parameter σ_i^2 is a strictly increasing function of SNR for $1 \leq i \leq M-1$, and

$$\lim_{\text{SNR} \rightarrow \infty} \sigma_i^2 = \begin{cases} \frac{MT_c^2}{2} \frac{1}{\gamma_s \beta} = \frac{MT_c^2}{2\gamma_n}, & i \leq 0 \\ \frac{iT_c^2}{2} \frac{1}{\gamma_s} + \frac{(M-i)T_c^2}{2} \frac{1}{\gamma_s \beta} \\ = \frac{MT_c^2}{2\gamma_n} + \frac{kT_c^2(\beta-1)}{2\gamma_n}, & 1 \leq i \leq M-1. \end{cases} \quad (38)$$

Thus, the probability of false alarm is a nondecreasing function of SNR that is strictly increasing if $\beta > 1$. And as the signal-to-noise ratio increases, the probability of false alarm approaches a limiting value determined by (32) and (38). This is illustrated in Fig. 2 for a combination of DS chip waveform and IF filter that results in $\beta = 2.08$. The Doppler shift of the received signal is zero. As in all the examples in this section, the length of the acquisition preamble is 400 chips, the false-alarm processing interval is 1000 chips, and the acquisition threshold is chosen to yield the smallest possible probability of not acquiring for a signal-to-noise ratio of 16 dB. If the signal-to-noise ratio is small, the probability of false alarm is given by $P_{fa} = 5.7 \times 10^{-4}$. As the SNR increases, the probability of false alarm increases to a limiting value of 4.0×10^{-2} .

The probability of miss depends on μ and σ_M , and from (35) and (36) it is seen that μ is an increasing function of SNR and σ_M is a decreasing function of SNR. One cannot infer from this a relationship between the probability of miss and SNR that is expressed as simply as the relationship between the probability of false alarm and SNR. Indeed, if for sufficiently low values of SNR the value of μ is very small and σ_M is very large, the probability of miss is a locally increasing function of SNR. In any practical application, however, there is some smallest value of SNR (denoted SNR_{\min}) for which it is necessary to achieve a low probability of not acquiring, and a low probability of miss cannot be achieved unless the threshold η is less than μ^2 for $\text{SNR} = \text{SNR}_{\min}$. If $\eta \leq \mu^2$ for $\text{SNR} = \text{SNR}_{\min}$, it follows from (33) that the probability of miss is a decreasing function of SNR for $\text{SNR} \geq \text{SNR}_{\min}$. This condition is satisfied in all circumstances of practical interest. Indeed, in many circumstances, the probability of miss is a decreasing function of SNR for an even wider range of values of SNR. This is illustrated in Fig. 2 for $\beta = 2.08$.

Suppose a reasonable acquisition threshold is chosen. For a sufficiently small value of SNR, the probability of miss is approximately one and the probability of false alarm is less than one. Thus the probability of miss dominates the probability of not acquiring for small values of SNR. As SNR approaches infinity, however, the probability of miss approaches zero and the probability of false alarm increases toward its nonzero limiting value. Thus the probability of false alarm dominates the probability of not acquiring for large values of SNR, and the probability of not acquiring is a locally increasing function of SNR. Thus the probability of not acquiring is a nonmonotonic function of SNR. This is illustrated in Fig. 3, in which the proba-

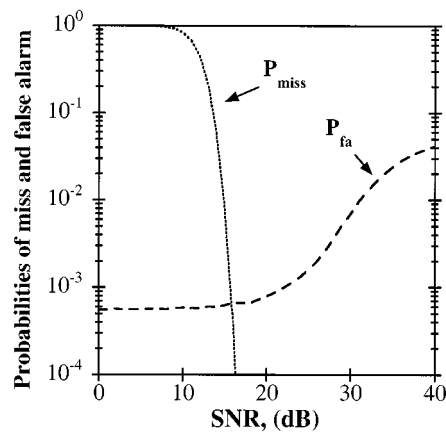


Fig. 2. Probabilities of miss and false alarm for $\beta = 2.08$ and a constant acquisition threshold. ($M = 400$, $Q = 1000$, $D_{T_c} = 0$.)

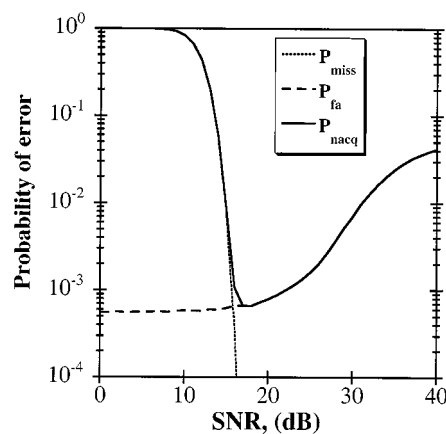


Fig. 3. Probabilities of miss, false alarm, and not acquiring for $\beta = 2.08$ and a constant acquisition threshold. ($M = 400$, $Q = 1000$, $D_{T_c} = 0$.)

bility of not acquiring is shown for a Doppler spread of zero if $\beta = 2.08$. The probability of miss and the probability of false alarm are also shown to illustrate that the former determines the performance if the signal-to-noise ratio is small and that the latter determines performance if the signal-to-noise ratio is large.

Nonmonotonicity as a function of SNR is exhibited by the probability of not acquiring for any value of β greater than one. This is illustrated in Fig. 4, in which the performance is shown for a Doppler shift of zero and several values of β . (Even though $\beta = 1.0$ is not achievable with a time-limited chip waveform, it is included for comparison.) The use of a sixth-order Butterworth IF filter and the matched filter in the acquisition stage results in $\beta = 2.5$ if $f_B = 1.25/T_c$, and it results in $\beta = 3.0$ if $f_B = 1.5/T_c$. If instead the IF filter is matched to the chip waveform and the filter in the acquisition stage is given by (9), $\beta = 1.5$ if the chip waveform is rectangular and $\beta = 2.08$ if the chip waveform is given by (21). Performance is shown in Fig. 4 for values of β including 1.0, 1.5, 2.08, 2.5, and 3.0. The threshold for each receiver is optimized to minimize P_{nacq} if $\text{SNR} = 16$ dB, and the resulting thresholds (normalized with respect to $M^2 T_c^2 / \gamma_s$) are 0.037 25, 0.025 25, 0.018 25, 0.015 25, and 0.013, respectively. It is seen that the severity of the nonmonotonicity increases as β increases. The nonmonotonicity is

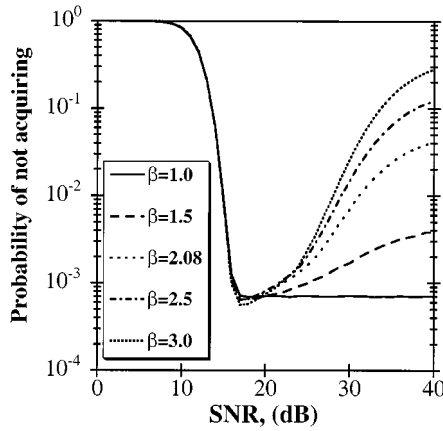


Fig. 4. Probability of not acquiring for several values of β , each with a constant acquisition threshold. ($M = 400$, $Q = 1000$, $D_{Tc} = 0$.)

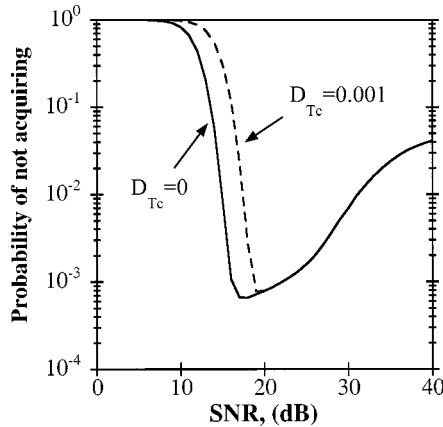


Fig. 5. Probability of not acquiring for $\beta = 2.08$ and a constant acquisition threshold. ($M = 400$, $Q = 1000$.)

exhibited even for a receiver that employs a chip-matched IF filter, however, since $\beta > 1$.

It is seen from (35)–(37) that the value of μ is a decreasing function of the Doppler shift in the received signal, but the Doppler shift does not affect the values of σ_i , $i \leq M$. Thus, the probability of false alarm does not depend on the Doppler shift, but the probability of miss (and consequently the probability of not acquiring) increases as the Doppler shift increases. This is illustrated in Fig. 5, in which the probability of not acquiring is shown for a receiver with $\beta = 2.08$ and for Doppler shifts of zero and 0.001. If the signal-to-noise ratio is small, the performance is nearly 3 dB poorer with the higher Doppler shift, since the probability of miss dominates in that region. If the signal-to-noise ratio is large, however, the probability of false alarm dominates performance and the performance does not depend on the Doppler shift.

It also follows from (35)–(37) that the value of γ_s affects the performance directly only as a scaling factor in the parameters μ^2 and σ_i^2 , $i \leq M$. For a given value of β , different values of γ_s result in the same performance as a function of SNR and D_{Tc} if the acquisition threshold is scaled in inverse proportion to γ_s . Thus it is unnecessary to specify the value of γ_s in any of the discussion above since the acquisition threshold is expressed as a quantity normalized with respect to $1/\gamma_s$.

VI. OPTIMIZATION OF THE ACQUISITION THRESHOLD

In the previous section, it is shown that the acquisition threshold that minimizes the probability of not acquiring for a given signal-to-noise ratio can result in poorer acquisition performance at higher signal-to-noise ratios. This fact is problematic for the design of the acquisition stage in the receiver, since it is usually desirable to select design parameters that guarantee a certain level of performance over a range of channel conditions. Perhaps the most natural design criterion is to select the threshold for the acquisition algorithm that results in the smallest possible worst-case probability of not acquiring over all values of the signal-to-noise ratio above a specified minimum value. If the smallest signal-to-noise ratio of interest is denoted SNR_{\min} , the optimal threshold based on this criterion is given by

$$\eta_{\text{opt}} = \arg \min_{\eta} \hat{P}_{\text{nacq}}(\eta)$$

where

$$\hat{P}_{\text{nacq}}(\eta) = \max_{\lambda \geq \text{SNR}_{\min}} \{P_{\text{nacq}}(\eta)|_{\text{SNR}=\lambda}\} \quad (39)$$

and $P_{\text{nacq}}(\eta)|_{\text{SNR}=\lambda}$ is the probability of not acquiring if the threshold is η and the SNR is λ .

The characterization of the acquisition performance in (32)–(37) does not lend itself to tractable evaluation of the optimal acquisition threshold. Instead, it is necessary to employ an exhaustive search over all possible thresholds and all signal-to-noise ratios in the range $\text{SNR} \geq \text{SNR}_{\min}$ in order to find the optimal threshold. Thus it is desirable to find a simpler procedure that produces an acquisition threshold that comes close to satisfying the criterion for the optimal threshold.

It is noted in Section III that for a given threshold, the largest probability of false alarm occurs if $\text{SNR} = \infty$. Thus the largest probability of false alarm for the range of channels specified by $\text{SNR} \geq \text{SNR}_{\min}$ also occurs if $\text{SNR} = \infty$. If the threshold is η , the worst-case value of P_{fa} is denoted by

$$\hat{P}_{\text{fa}}(\eta) = P_{\text{fa}}(\eta)|_{\text{SNR}=\infty}.$$

Similarly, if $\eta \leq \mu^2$ for $\text{SNR} = \text{SNR}_{\min}$, the worst-case probability of miss occurs if $\text{SNR} = \text{SNR}_{\min}$, and it is denoted by

$$\hat{P}_{\text{miss}}(\eta) = P_{\text{miss}}(\eta)|_{\text{SNR}=\text{SNR}_{\min}}.$$

(The upper bound on the threshold is satisfied for any threshold that results in reasonable performance for $\text{SNR} = \text{SNR}_{\min}$.)

Suppose that η_{sub} denotes the acquisition threshold chosen to minimize the maximum of $\hat{P}_{\text{fa}}(\eta)$ and $\hat{P}_{\text{miss}}(\eta)$, i.e.,

$$\eta_{\text{sub}} = \arg \min_{\eta} \hat{P}_{\text{sub}}(\eta)$$

where

$$\hat{P}_{\text{sub}}(\eta) = \max \left\{ \hat{P}_{\text{fa}}(\eta), \hat{P}_{\text{miss}}(\eta) \right\}. \quad (40)$$

Since \hat{P}_{fa} is a decreasing function of η and \hat{P}_{miss} is an increasing function of η , η_{sub} is unique for a given value of SNR_{\min} . Furthermore, since the miss and false-alarm probabilities are continuous functions of the threshold, $\hat{P}_{\text{fa}}(\eta_{\text{sub}}) = \hat{P}_{\text{miss}}(\eta_{\text{sub}})$. If $\eta_{\text{sub}} \geq \eta_{\text{opt}}$

$$\hat{P}_{\text{fa}}(\eta_{\text{opt}}) \geq \hat{P}_{\text{fa}}(\eta_{\text{sub}}).$$

If $\eta_{\text{sub}} \leq \eta_{\text{opt}}$

$$\hat{P}_{\text{miss}}(\eta_{\text{opt}}) \geq \hat{P}_{\text{miss}}(\eta_{\text{sub}}) = \hat{P}_{\text{fa}}(\eta_{\text{sub}}).$$

If $\min\{\eta_{\text{opt}}, \eta_{\text{sub}}\} \leq \mu^2$ for $\text{SNR} = \text{SNR}_{\text{min}}$, the worst-case probability of not acquiring that results with the optimal acquisition threshold is bounded by

$$\begin{aligned} \hat{P}_{\text{nacq}}(\eta_{\text{opt}}) &= \max_{\text{SNR} \geq \text{SNR}_{\text{min}}} [P_{\text{fa}}(\eta_{\text{opt}}) + P_{\text{miss}}(\eta_{\text{opt}}) \\ &\quad - P_{\text{fa}}(\eta_{\text{opt}})P_{\text{miss}}(\eta_{\text{opt}})] \\ &\geq \max_{\text{SNR} \geq \text{SNR}_{\text{min}}} [\max\{P_{\text{fa}}(\eta_{\text{opt}}), P_{\text{miss}}(\eta_{\text{opt}})\}] \\ &= \max\{\hat{P}_{\text{fa}}(\eta_{\text{opt}}), \hat{P}_{\text{miss}}(\eta_{\text{opt}})\} \\ &\geq \hat{P}_{\text{fa}}(\eta_{\text{sub}}) \end{aligned}$$

and the worst-case probability of not acquiring that results with the suboptimal acquisition threshold is bounded by

$$\begin{aligned} \hat{P}_{\text{nacq}}(\eta_{\text{sub}}) &= \max_{\text{SNR} \geq \text{SNR}_{\text{min}}} [P_{\text{fa}}(\eta_{\text{sub}}) + P_{\text{miss}}(\eta_{\text{sub}}) \\ &\quad - P_{\text{fa}}(\eta_{\text{sub}})P_{\text{miss}}(\eta_{\text{sub}})] \\ &\leq \max_{\text{SNR} \geq \text{SNR}_{\text{min}}} [P_{\text{fa}}(\eta_{\text{sub}}) + P_{\text{miss}}(\eta_{\text{sub}})] \\ &\leq \hat{P}_{\text{fa}}(\eta_{\text{sub}}) + \hat{P}_{\text{miss}}(\eta_{\text{sub}}) \\ &= 2\hat{P}_{\text{fa}}(\eta_{\text{sub}}). \end{aligned}$$

Thus

$$\hat{P}_{\text{nacq}}(\eta_{\text{sub}}) \leq 2\hat{P}_{\text{nacq}}(\eta_{\text{opt}}). \quad (41)$$

The condition that $\min\{\eta_{\text{opt}}, \eta_{\text{sub}}\} \leq \mu^2$ for $\text{SNR} = \text{SNR}_{\text{min}}$ holds for any situation of practical interest. Thus, a simple method requiring the evaluation of performance for only two channels, one with $\text{SNR} = \infty$ and the other with $\text{SNR} = \text{SNR}_{\text{min}}$, yields an acquisition threshold that results in a nearly optimal worst-case probability of not acquiring over the entire range of values of interest for the signal-to-noise ratio.

To illustrate the effectiveness of the suboptimal threshold-selection method, consider the system with a 400-chip preamble, a false-alarm processing interval of 1000 chips, a DS chip waveform and IF filter that result in $\beta = 2.08$, and a Doppler shift of zero. Suppose it is desired to minimize the worst-case probability of not acquiring over all values of the signal-to-noise ratio greater than or equal to 16 dB. Thus $\text{SNR}_{\text{min}} = 16$ dB. The threshold η_{opt} that minimizes the worst-case probability of not acquiring is the one that minimizes the objective function given by (39). In contrast, the threshold η_{sub} is the one that minimizes the objective function given by (40). Both objective functions for this example are shown in Fig. 6 as a function of the threshold. The value of $\hat{P}_{\text{nacq}}(\eta)$ is slightly greater than the value of $\hat{P}_{\text{sub}}(\eta)$ for any value of η , but the difference is so small that the plots of the two functions are indistinguishable in the figure. The function $\hat{P}_{\text{nacq}}(\eta)$ is minimized if $\eta = 0.02368(\gamma_s/M^2T_c^2)$, and $\hat{P}_{\text{sub}}(\eta)$ is minimized if $\eta = 0.02367(\gamma_s/M^2T_c^2)$. The resulting performance is virtually identical if either of the two thresholds is used, and it is shown for both thresholds in Fig. 7. In this example, the penalty in performance that results from using η_{sub} rather than η_{opt} is much less than is suggested by the bound given in (41).

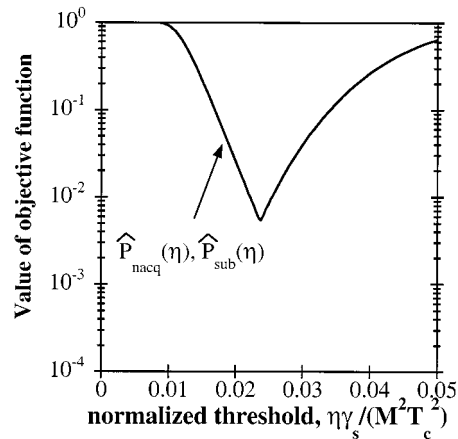


Fig. 6. Objective functions for determining $\eta_{\text{opt}}, \eta_{\text{sub}}$. ($\beta = 2.08, M = 400, Q = 1000$.)

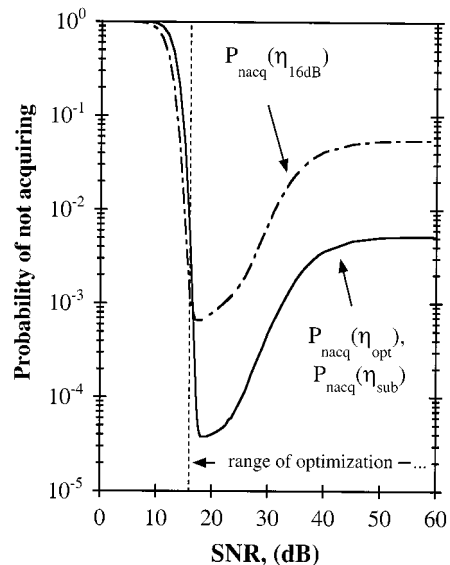


Fig. 7. Probability of not acquiring for $\beta = 2.08$ with $\eta_{\text{opt}}, \eta_{\text{sub}}$, and $\eta_{16 \text{ dB}}$. ($M = 400, Q = 1000, D_{T_c} = 0$.)

Indeed, the suboptimal threshold-selection method yields a threshold that is virtually the same as the optimal threshold, and the resulting performance is essentially optimal.

The results in Fig. 7 also illustrate the effect of selecting the threshold based on the performance over a range of signal-to-noise ratios rather than for a single value of SNR. The performance that is obtained if the threshold is equal to η_{opt} or η_{sub} is compared with the performance that is obtained if the threshold is selected to optimize performance for $\text{SNR} = 16$ dB. The latter threshold is denoted $\eta_{16 \text{ dB}}$. If $\text{SNR} = 16$ dB, the probability of not acquiring is 1.0×10^{-3} if $\eta = \eta_{16 \text{ dB}}$ but it is 5.5×10^{-3} if $\eta = \eta_{\text{opt}}$ or $\eta = \eta_{\text{sub}}$. But the worst-case probability of not acquiring over the range $\text{SNR} \geq 16$ dB decreases from 5.5×10^{-2} to 5.5×10^{-3} if η_{opt} or η_{sub} is used in place of $\eta_{16 \text{ dB}}$.

VII. CONCLUSION

The performance of a noncoherent acquisition algorithm is evaluated for a DS packet radio transmission employing

a fixed-length acquisition preamble. The acquisition algorithm is serial, and it is based on a matched-filter energy-threshold-crossing detector. The analysis accounts for differences in the frequency references of the transmitter and the receiver as well as Doppler shifts resulting from the mobility of the radios. It also accounts for the effect of the intermediate-frequency filter and the subsequent AGC system. The complex interdependence among the AGC system, the channel conditions, and the acquisition threshold in determining the performance of the acquisition technique is illustrated by several examples for which the probability of not acquiring is a markedly nonmonotonic function of the signal-to-noise ratio. A suboptimal method is presented for selecting an acquisition threshold that results in robust performance over a wide range of channel conditions. It is shown that use of this suboptimal threshold yields performance close to that obtained with the optimal threshold.

REFERENCES

- [1] TIA/EIA Standard, "Mobile station-base station compatibility standard for dual-mode wideband spread spectrum cellular system," Telecommunication Industry Association/Electronics Industry Association Interim Standard, Washington, D.C., TIA/EIA-95-B, 1999.
- [2] J. Jubin and J. D. Tornow, "The DARPA packet radio network protocols," *Proc. IEEE*, vol. 75, pp. 21–32, Jan. 1987.
- [3] D. V. Sarwate and M. B. Pursley, "Crosscorrelation properties of pseudorandom and related sequences," *Proc. IEEE*, vol. 68, pp. 593–619, May 1980.
- [4] M. K. Simon, J. K. Omura, R. A. Scholtz, and B. K. Levitt, *Spread Spectrum Communications Handbook*, revised ed. New York: McGraw-Hill, 1994.
- [5] A. Polydoros and C. L. Weber, "A unified approach to serial search spread-spectrum code acquisition—Part I: General theory," *IEEE Trans. Commun.*, vol. COM-32, pp. 540–549, May 1984.
- [6] U. Madhow and M. B. Pursley, "Acquisition in direct-sequence spread-spectrum communication networks: An asymptotic analysis," *IEEE Trans. Inform. Theory*, vol. 39, pp. 903–912, May 1993.
- [7] C. R. Cahn, "Spread spectrum applications and state-of-the-art equipments," in *Proc. AGARD-NATO Lecture Series, Spread Spectrum Communications*, Bolkesjø, Norway, May 1973, p. 5.
- [8] A. Polydoros and C. L. Weber, "A unified approach to serial search spread-spectrum code acquisition—Part II: A matched filter receiver," *IEEE Trans. Commun.*, vol. COM-32, pp. 550–560, May 1984.
- [9] D. E. Cartier, "Partial correlation properties of pseudonoise (PN) codes in noncoherent synchronization/detection schemes," *IEEE Trans. Commun.*, vol. COM-24, pp. 898–903, Aug. 1976.
- [10] U. Cheng, W. J. Hurd, and J. I. Statman, "Spread-spectrum code acquisition in the presence of Doppler shift and data modulation," *IEEE Trans. Commun.*, vol. 38, pp. 241–250, Feb. 1990.
- [11] K. K. Chawla and D. V. Sarwate, "Acquisition of PN sequences in chip synchronous DS/SS systems using a random sequence model and the SPRT," *IEEE Trans. Commun.*, vol. 42, pp. 2325–2334, June 1994.
- [12] B. Razavi, *RF Microelectronics*. Upper Saddle River, NJ: Prentice-Hall, 1998.
- [13] M. E. Van Valkenburg, *Analog Filter Design*. New York: CBS College, 1982.
- [14] B. Fristedt and L. Gray, *A Modern Approach to Probability Theory*. Boston, MA: Birkhäuser, 1997.

[15] M. Schwartz, W. R. Bennett, and S. Stein, *Communication Systems and Techniques*. New York: McGraw-Hill, 1966.



Daniel L. Noneaker (M'93) was born in Montgomery, AL, on December 10, 1957. He received the B.S. degree in mathematics (with high honors) from Auburn University, Auburn, AL, in 1977, the M.S. degree in mathematics from Emory University, Atlanta, GA, in 1979, the M.S. degree in electrical engineering from the Georgia Institute of Technology, Atlanta, in 1984, and the Ph.D. degree in electrical engineering from the University of Illinois at Urbana-Champaign in 1993.

Dr. Noneaker has industrial experience in both hardware and software design for communications systems. From 1979 to 1982, he was with Sperry-Univac, Salt Lake City, UT. From 1984 to 1988, he was with the Motorola Government Electronics Group, Scottsdale, AZ. He was a Research Assistant in the Coordinated Science Laboratory, University of Illinois, Urbana, from 1988 to 1993. Since 1993, he has been with the Department of Electrical and Computer Engineering, Clemson University, Clemson, SC, where he currently holds the position of Assistant Professor. He is currently engaged in research on wireless communications for both military and commercial applications with emphases on spread-spectrum communications, error-control coding for fading channels, and protocols for mobile radio networks. He has published several papers concerning the design and analysis of multiple-access systems for cellular telephony and data transmission.

Arvind R. Raghavan received the B.E. degree in electronics and telecommunications from Karnataka Regional Engineering College, Surathkal, India, in 1992 and the M.S. and Ph.D. degrees in electrical engineering from Clemson University, Clemson, SC, in 1996 and 1999, respectively.

He is currently with OPNET Technologies, Inc., Washington, DC, where he is involved in modeling network protocols and switch architectures. His research interests are in MAC protocols for WCDMA and broad-band wireless access systems.

Dr. Raghavan received the Harris Outstanding Graduate Researcher Award from Clemson University in 1999.



Carl W. Baum (S'87–M'92) was born in Pasadena, CA, in 1965. He received the B.S. degree in electrical engineering (with highest distinction) from the University of California, Los Angeles, in 1987 and the M.S. and Ph.D. degrees in electrical engineering from the University of Illinois, Urbana-Champaign, in 1989 and 1992, respectively.

He was a University of Illinois Fellow from 1987 to 1988. From 1987 to 1992, he held a Graduate Research Assistantship at the Coordinated Science Laboratory, University of Illinois, Urbana-Champaign. In 1992, he joined Clemson University, Clemson, SC, where he is currently an Associate Professor in electrical engineering. His current research interests are in the general areas of detection theory and communications theory with emphasis on spread-spectrum communications.

Dr. Baum is a member of Tau Beta Pi, Eta Kappa Nu, and Phi Eta Sigma. He received the Robert Chien Memorial Award from the University of Illinois for excellence in research in the field of electrical and computer engineering in 1992. In 1996, he received the IEEE Browder J. Thompson Prize Award for the outstanding paper by authors under 30 years of age.